JOURNAL OF GEOPHYSICAL RESEARCH, VOL. 104, NO. B8, PAGES 17,975–17,993, AUGUST 10, 1999

Shear wave splitting in the Appalachians and the Urals: A case for multilayered anisotropy

Vadim Levin

Department of Geology and Geophysics, Yale University, New Haven, Connecticut

William Menke

Lamont-Doherty Earth Observatory of Columbia University, Palisades, New York

Jeffrey Park

Department of Geology and Geophysics, Yale University, New Haven, Connecticut

Abstract. Observations of shear wave splitting in the northeastern U.S. Appalachians and in the foredeep of the Urals vary significantly with the back azimuth and incidence angle of the incoming phase. These variations suggest two or more layers within the upper mantle with different anisotropic properties. Synthetic seismograms for simple multilayered anisotropic structures show that shear wave splitting parameters tend to vary substantially with the direction of approach. Relying on a subset of back-azimuth and incidence angle may strongly bias the model inferred, especially if the observations are averaged. On the other hand, the azimuthal splitting pattern provides additional constraints on vertical or lateral variation of anisotropic properties in the Earth. Using a new error estimation technique for splitting, we find that individual measurements from broadband data have errors of the order of $\delta\phi = 3°$-$7°$for the fast direction and $0.1 - 0.2$ s for the delay of split shear waves. The azimuthal variation of splitting parameters is broadly consistent throughout the Appalachian terranes in the northeast United States, especially for two long-running stations in the northeast United States, HRV (Harvard, Massachusetts) and PAL (Palisades, New York). Observations can be separated into two distinct populations, with mean fast-axis azimuths of N60°E±4°and N119°E±2°. Delay values within each population range from near zero to ∼1 s. Azimuthal splitting variation for ARU (Arti, Russia) in the foredeep of Uralian mountains is characterized by sharp transitions between different groups of observations. Using synthetic seismograms in simple structures, we develop one-dimensional anisotropic models under stations HRV and ARU. The model for HRV includes two layers of anisotropic material under an isotropic crust, with fast-axis azimuths N53°E and N115°E for the bottom and the top layers, respectively. The model for the upper mantle under ARU includes a layer with a fast-axis at N50°E atop a layer with fast axis azimuth N90°E. Our modeling confirms the need for a layer of strong anisotropy with a slow axis of symmetry in the lower crust under ARU, reported by *Levin and Park* [1997a]. Our results suggest that both Urals and Appalachians possess a relict anisotropy in the tectosphere, associated with past continental collision and accretion, underlain by anisotropy with orientation similar to the local absolute plate motion, suggesting an asthenospheric component to the signal.

1. Introduction

Seismic anisotropy, the dependence of seismic velocity on the direction of propagation, is a common feature of modern global seismic velocity models [*Dziewonski and Anderson*, 1981] and a well-documented property of olivine, the mineral that composes the bulk of the upper mantle [*Crampin et al.*, 1984]. A prominent effect of seismic anisotropy is the so-called splitting of shear waves. Unlike the two shear modes in isotropic materials, which have equal phase velocities, the two corresponding modes in anisotropic materials have different

Paper number 1999JB900168.
0148-0227/99/1999JB900168$09.00

velocities. As it enters an anisotropic region, a single linearly polarized shear wave pulse will split into two pulses of different velocity. The polarizations of these pulses are related to the projection of their propagation direction onto the axes of the anisotropic elastic tensor [*Aki and Richards,* 1981].

Shear wave splitting studies measure and describe the anisotropy of the Earth. One selects shear wave phases that are known to be linearly polarized prior to entering the anisotropic study region, and measures their particle motion after traversing the region. One seeks a coordinate rotation that separates the particle motion into distinct "fast" and "slow" pulses, each of identical shape and linearly polarized in mutually-perpendicular fast and slow directions. The delay between the two pulses is proportional to the strength of the anisotropic effect, which depends both on the intensity of seismic anisotropy and the length of the path within the anisotropic material. The axes of the rotated coordinate system provide information on the symmetry and orientation of the anisotropic elastic tensor.

In some simple cases, such as when the tensor has hexagonal symmetry with a horizontal symmetry axis, the orientation of the fast splitting axis is approximately parallel to the symmetry axis, regardless of propagation direction. This simplification is often assumed in studies of the upper mantle. Estimates of splitting time and fast-axis direction from many shear waves at a given station have been averaged to estimate anisotropic strength (i.e., delay time) and symmetry-axis azimuth for the mantle beneath that station [e.g., *Vinnik et al.*, 1995; *Barruol et al.*, 1997; *Wolfe and Silver*, 1998; M. J. Fouch et al., Shear wave splitting, continental keels, and patterns of mantle flow, submitted to *Journal of Geophysical Research*, 1999, hereinafter referred to as Fouch et al., submitted manuscript, 1999]. Such "station means" are useful in tectonic settings where uniformity of the fabric in the lithosphere is likely, e.g. on the ocean floor [*Wolfe and Solomon*, 1998] or in the wake of a hot spot [*Schutt et al.*, 1998].

Station means may be quite misleading, however, in cases where both the delay time and the fast direction vary significantly with the propagation direction. Such variation can occur when an anisotropy tensor is inclined from the vertical or has a more complicated symmetry or both (Figure 1). *Babuška et al.* [1993] discuss possible scenarios that involve an inclined orientation of hexagonal and orthorhombic anisotropic tensors. This possibility has also been considered by *Plomerova et al.*, [1996], *Levin et al.* [1996], *Hirn et al.* [1998], and others. Also, a combination of two or more layers of anisotropy with hexagonal symmetry and horizontal symmetry axes leads to a systematic variation of the splitting parameters with the polarization of the incoming shear wave [*Silver and Savage*, 1994; *Vinnik et al.*, 1994]. For vertically incident shear waves a simple analytic expression describes the variation of splitting parameters in a simple two-layer model, predicting a $\pi/2$ periodicity. Two-layer models with horizontal axis anisotropy are often invoked to explain back azimuth variations in splitting parameters [e.g., *Ozalaybey and Savage*, 1994; *Russo and Silver*, 1994; *Granet et al.*, 1998].

In this paper we demonstrate that the fast direction

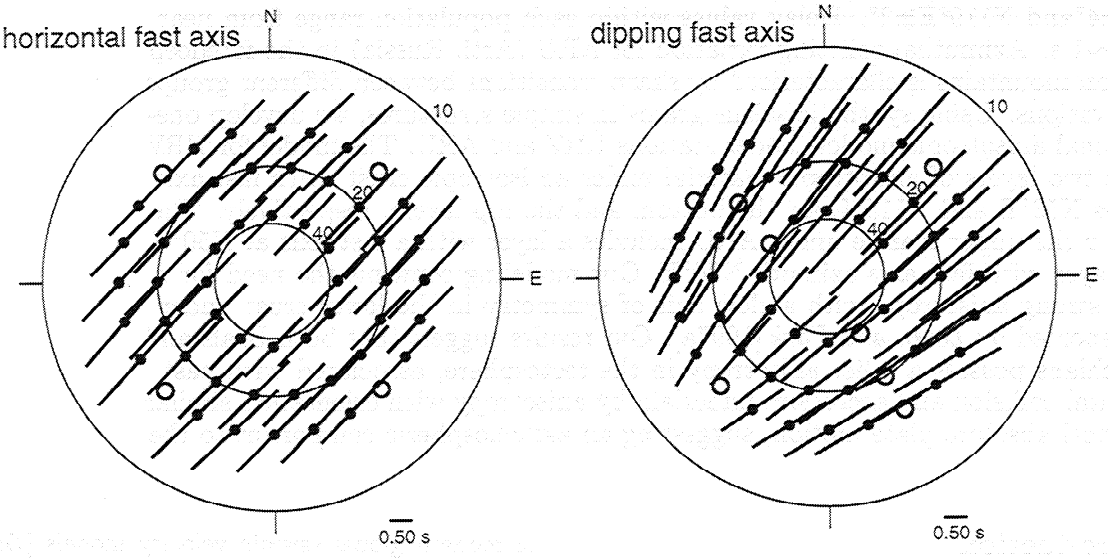

Figure 1. Shear-wave fast direction and delay for SKS waves received at a hypothetical station from a variety of directions and apparent velocities (in km/s). Data are shown as a bar centered on the nominal back azimuth and apparent velocity, with the bar's orientation parallel to the azimuth of the the fast direction and its length proportional to the delay. Near-zero delays are plotted with open circles. (left) For an Earth model with a single hexagonally anisotropic layer with horizontal symmetry axis overlying an isotropic half-space; (right) for a model in which the symmetry axis plunges 45°. Note that the splitting parameters vary most slowly in the horizontal case.

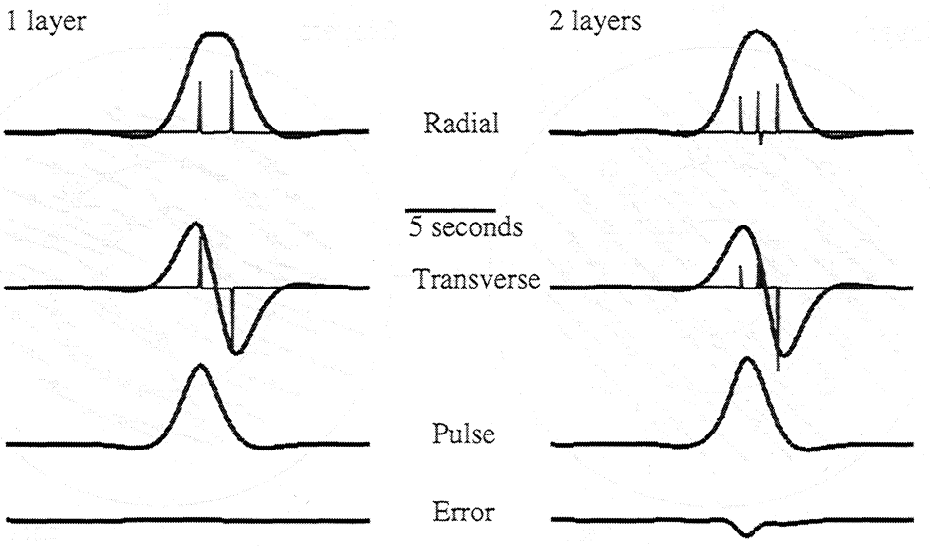

Figure 2. Synthetic SKS phases for two earth models. (right) Two 50 km hexagonally-anisotropic layers overlying an isotropic halfspace. The symmetry axis is horizontal in both layers, and has an azimuth of N30°E in the top layer and N60°E in the bottom layer. (left) One 100 km anisotropic layer overlying an isotropic halfspace. The anisotropic tensor is the arithmetic mean of the tensors in the two-layer case. Radial and transverse horizontal component synthetic seismograms (bold) are computed by convolving the impulse response functions (solid) with a pulse that has a bandwidth similar to typical SKS phases. This SKS pulse (N270°E, 20 km/s) is reconstructed using apparent splitting parameters computed by the cross correlation method. Note that the two layer case has the larger error.

and delay associated with shear waves that sample the Earth's upper mantle beneath two long-lived mountain belts vary strongly with shear wave propagation direction. We interpret these variations in terms of multilayered anisotropy, implying either complex deformation in a past collisional event or, more plausibly, a mix of active and fossil deformations.

The parameters of a split shear wave can be estimated by a grid search over possible time delays and fast-axis directions, and using some kind of goodness-of-fit criteria to select the "best" set of values. Two criteria have been used: (1) maximal similarity in the pulse shapes of the two rotated seismogram components, as quantified by cross correlation [e.g., *Bowman and Ando*, 1987; *Iidaka and Niu*, 1998]; and (2) that the reassembled "original" pulse has maximal rectilinearity, as quantified by the ratio of the rectilinear and elliptical motion [*Kosarev et al.*, 1984; *Silver and Chan*, 1991]. These two methods give the same results when tested on nearly noise-free data. Owing to their different treatment of noise and to complications induced by multilayered anisotropy, "cross correlation" and "rectilinearity" measures can give substantially different results when applied to noisy data.

If the anisotropic material is homogeneous, an observed split shear wave is exactly the sum of two pulses of different polarization, one delayed with respect to the other. If, in contrast, the anisotropic material consists of several layers (or, more generally, three-dimensional (3-D) domains) of different anisotropy, then the observed seismogram has a more complicated form, with a sequence of pulses corresponding to mode conversions from the various layer interfaces. In general, no rotation exists in which one component of the seismogram is exactly a delayed version of the other (Figure 2). Given a high-quality broadband waveform with no interfering seismic signals, these conversions could perhaps be individually identified and modeled. Unfortunately, most SKS data in studies of the upper mantle are low-passed, and resolving closely spaced sequence of pulses is problematic.

Our approach is to retain the two-parameter (fast direction and delay) description for shear wave propagation in anisotropic media but to recognize that this is an "apparent" measurement, without exact correspondence to an underlying physical process. This approach was introduced by *Silver and Savage* [1994] for the case of two anisotropic layers with horizontal symmetry axes and more recently expanded to the case of a smoothly varying medium by *Rumpker and Silver* [1998]. The apparent splitting parameters (Figure 3) contain significant information about the anisotropic medium. Most importantly, the apparent splitting parameters are different from what one would expect for a homogeneous medium with the same "mean" anisotropy, so that some information on the depth dependence of the anisotropy is preserved. Unfortunately, owing to interference between the mode conversions, the measured values of the

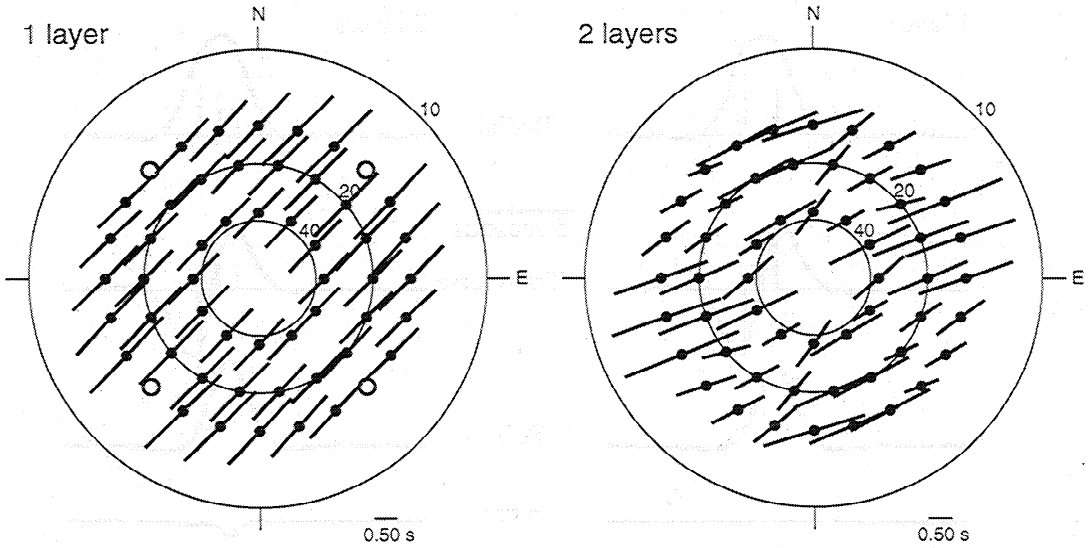

Figure 3. Apparent splitting parameters for SKS waves received at a hypothetical station. (right) For an Earth model with two 50 km hexagonally-anisotropic layers overlying an isotropic half-space. The symmetry axis is horizontal in both layers and has an azimuth of N30°E in the top layer and N60°E in the bottom layer. (left) For an Earth model with one 100 km anisotropic layer overlying an isotropic half-space. The anisotropic tensor is the arithmetic mean of the tensors in the two-layer case. Splitting parameters are computed by the cross correlation method from synthetic SKS phases. Note that the two-layer case has the more complex pattern.

apparent parameters are somewhat sensitive to the frequency band of the seismic data (Figure 4). *Rumpker and Silver* [1998] show that even for a case of vertical incidence in a flat-layered model with horizontal axes of hexagonal symmetry, apparent splitting parameters exhibit strong dependence on the ratio between the cumulative splitting effect of the medium and the frequency content of the shear wave. This sensitivity does not present any fundamental problem when modeling the apparent splitting. One simply compares observed apparent values with predicted ones that have been computed from synthetic seismograms with the same frequency content. However, it makes difficult the comparison of data collected by different authors using different processing schemes.

In this paper we measure apparent splitting parameters at a few locations within two Paleozoic mountain belts: the Appalachians and the Urals. We focus on the anisotropic structure of the upper mantle and so use mostly SKS and $SKKS$ phases. We mainly use stations with long duration of operation, and thus we are able to obtain measurements from a wide variety of azimuths and angles of incidence. We show that the strong directional behavior of these data indicate that the upper mantle beneath these two mountain belts possesses multiple layers of different anisotropy.

2. Seismic Anisotropy in the Continental Lithosphere

Silver [1996] summarizes arguments, developed over the previous decade, that anisotropy is primarily a feature of the uppermost few hundred kilometers of the Earth. This view has been recently challenged by observations of seismic anisotropy near the core-mantle boundary [*Kendall and Silver*, 1996; *Garnero and Lay*, 1997] and within the transition zone [*Vinnik and Montagner*, 1996]. Nevertheless, the presence of seismic anisotropy within the lithosphere is well-documented.

The variety of mechanisms that produce anisotropy of seismic properties in the lithosphere centers on a handful of scenarios. In the upper crust the strongest influence is believed to be that of aligned cracks and/or pore spaces [*Babuška and Proš*, 1984], for which slower velocities are found for waves that propagate normal to the average crack plane. The aspect ratio of pore/cracks and type of fluid determine the extent and proportion of anisotropy [*Hudson*, 1981; *Crampin*, 1991]. Alternating thin isotropic layers of higher and lower velocity can also produce an overall anisotropic effect [*Backus*, 1962; *Helbig*, 1994], with the velocities slower normal to the bedding than along it. In the lower crust and the uppermost mantle, cracks are assumed to close in response to increasing overburden pressure [*Babuška and Proš*, 1984; *Kern et al.*, 1993], though field exposures of (formerly) deep-crustal fluid-filled cracks can be found [*Ague*, 1995]. In the absence of cracks and inclusions the lattice-preferred orientation (LPO) of mineral crystals is taken as the main cause of seismic anisotropy. Most minerals composing the bulk of the crust are anisotropic to some degree [*Babuška and Cara*, 1991], as are the olivine and orthopyroxene that predominate in the upper mantle anisotropy. Different deformation mechanisms can lead to the alignment of either the slow or the

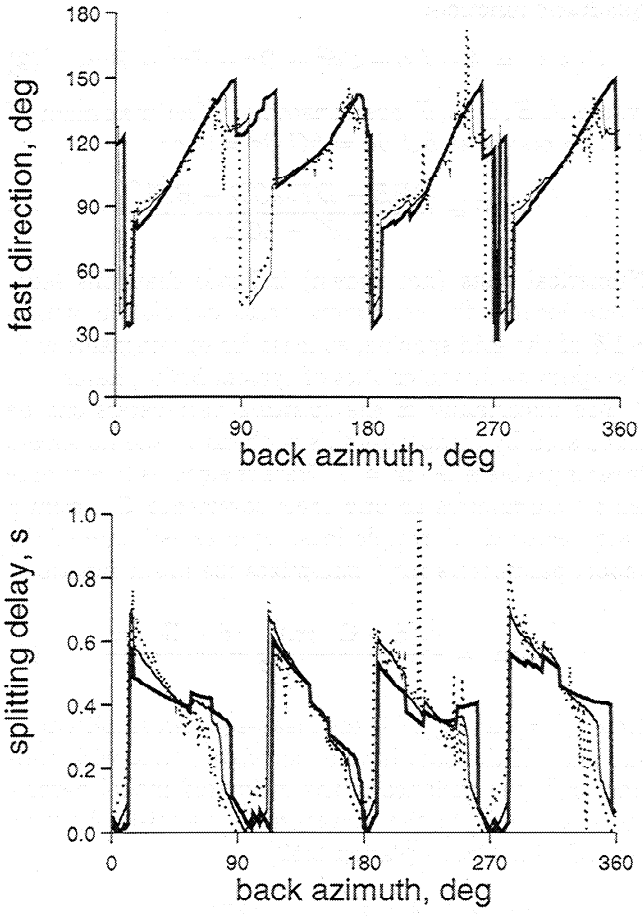

Figure 4. Influence of the filtering applied to the synthetic waveforms on the apparent splitting parameters. Waveforms are simulated in a two-layer model developed for station HRV (see Table 2). Apparent splitting parameters measured from waveforms with an upper spectral limits of 0.45 Hz (bold), 0.35 Hz (solid) and 0.15 Hz (dotted) are shown, with a lower limit of 0.05 Hz common for all. For all cases tested, the estimate of the apparent fast direction tends to vary greatly when the delay is the smallest. The lowest band pass (0.15Hz) gives most unstable results throughout.

fast crystallographic direction in olivine grains [*Nicolas et al.*, 1973; *Ribe*, 1992], but LPO caused by dislocation creep in the shallow mantle is commonly believed to lead to preferred alignment of the fast axis [*Zhang and Karato*, 1995].

It is natural to expect that strain-induced seismic anisotropy would be particularly prominent in plate boundary regions, where deformations are concentrated. World wide observations of shear wave splitting support this notion [*Silver*, 1996]. Present-day regions of active compression commonly have fast axis of seismic anisotropy aligned sub parallel to the strike of the orogen. One explanation for such orientation is the preferred alignment of slow axes of olivine along the direction of compression [*Nicolas et al.*, 1973]. *Vauchez and Nicolas* [1991] propose an alternative mechanism: preferred alignment of the olivine fast axes along the orogen as a result of concurrent strike-slip deformation commonly observed during mountain building.

Some stable continental interiors have anisotropic intensity equal, if not superior, to actively deforming regions, perhaps because many now-stable continental regions have experienced plate-boundary deformation in the past, and have retained a fossil deformation. Patterns of seismic anisotropy within stable continental masses may therefore record the tectonic history of these regions. Seismic stations examined in this work lie within two Paleozoic mountain belts, the Appalachians and the Urals. Both have been loci of continent-building accretionary episodes in early Paleozoic time. Both regions are presently embedded within stable continental region, the North American and Eurasian plates, respectively.

A number of shear wave splitting studies have examined the northeastern United States, using both permanent and temporary stations [e.g., *Silver and Chan*, 1991; *Fouch and Fischer*, 1995; *Levin et al.*, 1996; *Barruol et al.*, 1997; Fouch et al., submitted manuscript, 1999]. In most cases a single "average" set of parameters was reported for selected sites (Figure 5). The average of all values shown in the map may be treated as a "regional average" and comes out as delay $\tau \sim 0.9$s

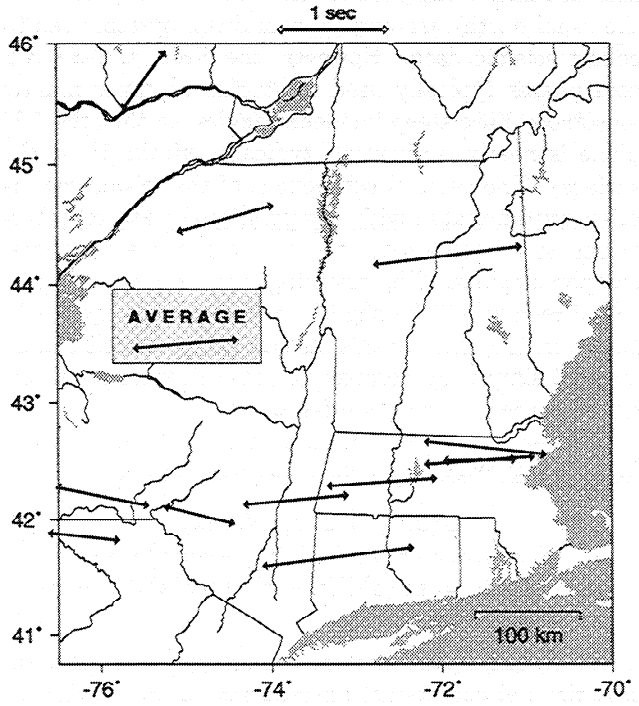

Figure 5. Map of NE Appalachian region, with "average" parameters of seismic anisotropy plotted at points where they were constrained by various workers. Arrow azimuths correspond to the fast directions determined for the particular site, and are scaled with estimated delay. (The compilation is from the "Anisotropy Resource Page" maintained by Derek Schutt (http://darkwing.uoregon.edu/~schuttd/aniso_source.html). Individual values are from *Silver and Chan* [1991], *Bostock and Cassidy* [1995], *Barruol et al.* [1997] and Fouch et al., submitted manuscript, (1999).

and a fast direction $\phi \sim 85°$ clockwise CW from north. *Helffrich et al.* [1994] reported average splitting parameters of ϕ = N68 °E and $\tau \sim 1$ s for station ARU (Arti, Russia), the station we examine in the foredeep of the Urals. It is interesting to note that in both the northeastern Appalachians and the central Urals, the fast axes of seismic anisotropy are often not parallel to the strike of the orogenic belt and thus do not follow the pattern reported in active-tectonic regions like the Pyrenees [*Vauchez and Nicolas*, 1991].

3. Splitting Parameters and Their Variance

Single seismogram estimates are needed to investigate the variation of splitting parameters with S wave propagation direction. We use the cross correlation method to find the parameters that best fit the model that the S wave is composed of two pulses of identical shape but orthogonal polarization, one delayed with respect to the other.

Let us suppose that the S wave polarization lies with the UV plane of a Cartesian UVW coordinate system. For weakly anisotropic material, such as the Earth's mantle, the propagation direction will then be nearly parallel to W. In general, one might need to establish the relationship between this coordinate system and the usual north-east-vertical coordinate system used to collect seismic data. However, the SKS and $SKKS$ core phases typically used in studies of upper mantle anisotropy have steep incidence angles, so that the UV plane is nearly horizontal (typically within 5° at the surface). The vertical component of the seismogram is often contaminated with compressional wave reverberations, so we believe it is best to use only the horizontal component data. The resulting measurement of splitting direction will be slightly biased by this approach. However, the effect of this bias on Earth models can be avoided simply by comparing these data to synthetic data oriented in the same fashion.

We seek to find a rotation ϕ in the UV plane and a delay τ that maximizes the cross correlation:

$$\begin{gathered} C(\phi,\tau) = \mathbf{u}^T\mathbf{v}/(Ns_u s_v) \\ u_i = u(\phi,t_i) = \cos(\phi)U(t_i) - \sin(\phi)V(t_i) \\ v_i = v(\phi,t_i) = \sin(\phi)U(t_i-\tau) + \cos(\phi)V(t_i-\tau) \end{gathered} \tag{1}$$

where s_u and s_v are the root-mean-square amplitudes of horizontal component seismograms $\mathbf{u}$ and $\mathbf{v}$, respectively, and $t_i = i\Delta t$, where Δt is the sampling interval of the seismogram. After grouping the splitting parameters into a vector $\mathbf{m} = [\phi,\tau]^T$, we denote the cross correlation as $C(\mathbf{m})$.

We estimate the best-fitting vector $\mathbf{m}^{\text{est}}$ using a coarse grid search followed by refinement with an interpolation algorithm. We use a grid spacing of Δt in τ and 5° in ϕ. We fit (using least squares) the cross correlation at the maximal node and its nearest neighbors with a biquadratic function:

$$C(\phi,\tau) = A + B\phi + C\phi^2 + D\tau + E\tau^2 + F\tau\phi \tag{2}$$

where $A, B, C, ..., F$ are constants. The maximum of $C(\phi,\tau)$ occurs at $\partial C\,\partial\phi = \partial C\,\partial\tau = 0$, or

$$\mathbf{m}^{\text{est}} = \frac{[2BE - DF, 2CD - BF]^T}{(F^2 - 4CE)} \tag{3}$$

Numerical tests (not shown) indicate that this technique locates the maximum cross correlation within ~1% of the grid spacing, at least for seismograms with the spectral characteristics of typical SKS phases.

The uncertainty of the splitting parameters can be calculated by comparing this problem to the linearized inverse problem $\mathbf{G}\cdot\mathbf{m} = \mathbf{d}$. Here the goal is to estimate model parameters $\mathbf{m}$ and their covariance $\mathbf{C}_m$ from a data vector $\mathbf{d}$. A simple least squares estimate of the model parameters $\mathbf{m}^{\text{est}}$ minimizes the misfit function:

$$E(\mathbf{m}) = \frac{\frac{1}{N}(\mathbf{d}-\mathbf{G}\cdot\mathbf{m})^T\cdot(\mathbf{d}-\mathbf{G}\cdot\mathbf{m})}{{s_d}^2} \tag{4}$$

Here ${s_d}^2 = (\mathbf{d}^T\cdot\mathbf{d})/N$ is the mean-squared amplitude of the data. If the data have uncorrelated error with variance ${\sigma_d}^2$, the variance of the estimated model parameters is related to the curvature of the misfit function [see *Menke*, 1989, equation 3.52]:

$$\mathbf{C}_m = \frac{\sigma_d^2}{N{s_d}^2}\left[\frac{1}{2}\nabla_m\nabla_m E\right]^{-1}\Bigg|_{\mathbf{m}=\mathbf{m}^{\text{est}}} \tag{5}$$

. Equation (5) quantifies the notion that narrow minima are associated with precise estimates. The ratio s_d/σ_d can be interpreted as the signal-to-noise ratio r_d.

We apply (5) to maximize the coherence between two seismograms $\mathbf{u}$ and $\mathbf{v}$, each of length N. The misfit function is

$$E(\mathbf{m}) = \frac{1}{2N}\left(\frac{\mathbf{u}}{s_u} - \frac{\mathbf{v}}{s_v}\right)^T\left(\frac{\mathbf{u}}{s_u} - \frac{\mathbf{v}}{s_v}\right) \tag{6}$$

where s_u and s_v are the root-mean-square amplitudes of $\mathbf{u}$ and $\mathbf{v}$, respectively. This definition of misfit is algebraically equivalent to $E = 1 - C$, where $C = \mathbf{u}^T\mathbf{v}/(Ns_u s_v)$ is the cross correlation between the two data series. The variance of $\mathbf{m}$ is given by

$$\mathbf{C}_m = -\frac{1}{Nr^2}\left[\frac{1}{2}\nabla_m\nabla_m C\right]^{-1}\Bigg|_{\mathbf{m}=\mathbf{m}^{\text{est}}} \tag{7}$$

where r is the signal-to-noise ratio (assumed the same on the two seismograms). We estimate the second derivative matrix by differentiating the quadratic interpolant (2) of the cross correlation $C(\phi,\tau)$.

The signal-to-noise ratio can be estimated from the value of C itself by assuming that deviations from perfect correlation are caused entirely by stochastic noise in the seismograms. Denoting this noise as $\mathbf{n}_u$ and $\mathbf{n}_v$

and $\mathbf{u}_o$ and $\mathbf{v}_o$ as noise-free seismic signals, we have

$$C = \frac{(\mathbf{u}_o + \mathbf{n}_u)^T(\mathbf{v}_o + \mathbf{n}_v)}{|\mathbf{u}_o + \mathbf{n}_u|^{\frac{1}{2}}|\mathbf{v}_o + \mathbf{n}_v|^{\frac{1}{2}}} \tag{8}$$

We assume that the noise-free $\mathbf{u}_o$ and $\mathbf{v}_o$ are scaled versions of each other. The expected value of the cross correlation is

$$< C >= \frac{< \mathbf{u}_o^T \mathbf{v}_o >}{\sqrt{< \mathbf{u}_o^T \mathbf{u}_o >}\sqrt{< \mathbf{v}_o^T \mathbf{v}_o >}[1 + r^{-2}]} = \frac{1}{[1 + r^{-2}]} \tag{9}$$

The estimated signal-to-noise ratio is thus $r = (C^{-1} - 1)^{-\frac{1}{2}}$.

Most time series are oversampled and thus have correlated noise. For this case, N in (3) must be replaced with the degrees of freedom $\nu < N$:

$$\mathbf{C}_m = -\left(\frac{1}{\nu r^2}\right)\left[\frac{1}{2}\nabla_m \nabla_m C\right]^{-1}\Big|_{\mathbf{m}=\mathbf{m}^{\mathbf{est}}} \tag{10}$$

The degrees of freedom can be estimated by computing the autocorrelation of the normalized misfit

$$\mathbf{e}(\mathbf{m}) = \frac{1}{\sqrt{2}}\left(\frac{\mathbf{u}(\mathbf{m}^{\mathbf{est}})}{s_u} - \frac{\mathbf{v}(\mathbf{m}^{\mathbf{est}})}{s_v}\right) \tag{11}$$

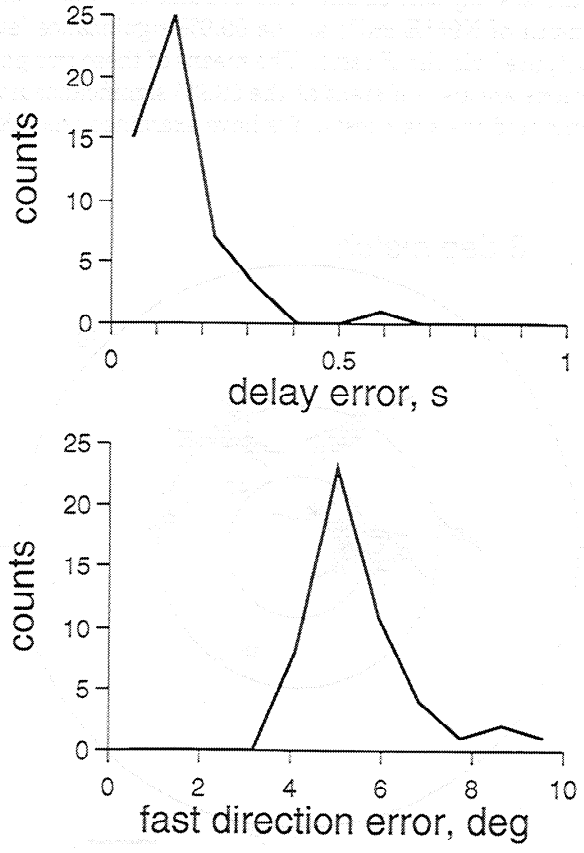

Figure 6. Histograms of single seismogram splitting parameter errors for HRV data. (top) One σ error in delay time. (bottom) One σ error in fast direction azimuth.

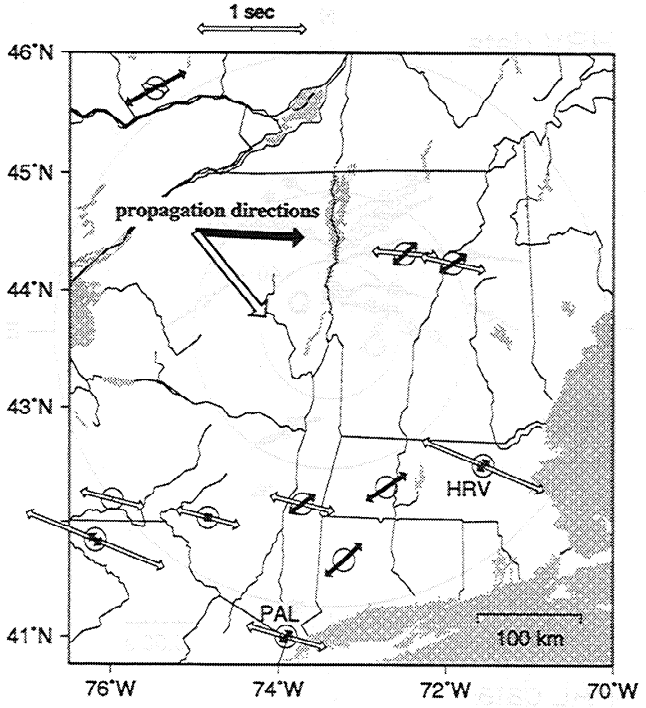

Figure 7. Map of NE Appalachian region showing shear wave splitting data for two earthquakes with different propagation directions (large one-sided arrows) observed in 1995. Splitting azimuth and delay are shown at each station as two-sided arrows aligned with the fast direction and scaled with delay. Symbols are coded by event, solid for one and open for the other. Note that splitting directions for the two events are quite different, yet are fairly consistent across the region for each event.

The ratio N/ν is approximately the width of the main peak in the autocorrelation of $\mathbf{e}(\mathbf{m}^{\mathbf{est}})$.

We have tested this method of computing covariance against Monte Carlo simulations using synthetic SKS phases that have prescribed signal-to-noise ratios in the 1:1 to 100:1 range. The results (not shown) indicate that the above methodology yields accurate estimates of variance. Standard deviations generally agree with Monte Carlo results to within 20-30%. Standard deviations are typically $3° - 7°$ for the fast axis azimuth and $\sigma_\tau \sim 0.1 - 0.2$ s for data used in this study (Figure 6).

4. Shear Wave Splitting in NE Appalachians

Figure 7 shows the pattern of SKS shear wave splitting for two earthquakes with different back azimuths (westerly and northwesterly), observed at all available seismic stations in the NE Appalachian region. The observed shear wave fast directions differ for the two back azimuths. The event with westerly back azimuth has a northeasterly fast direction, while the event with the northwesterly back azimuth has an easterly fast direction. The fast direction appears to be a rapidly varying

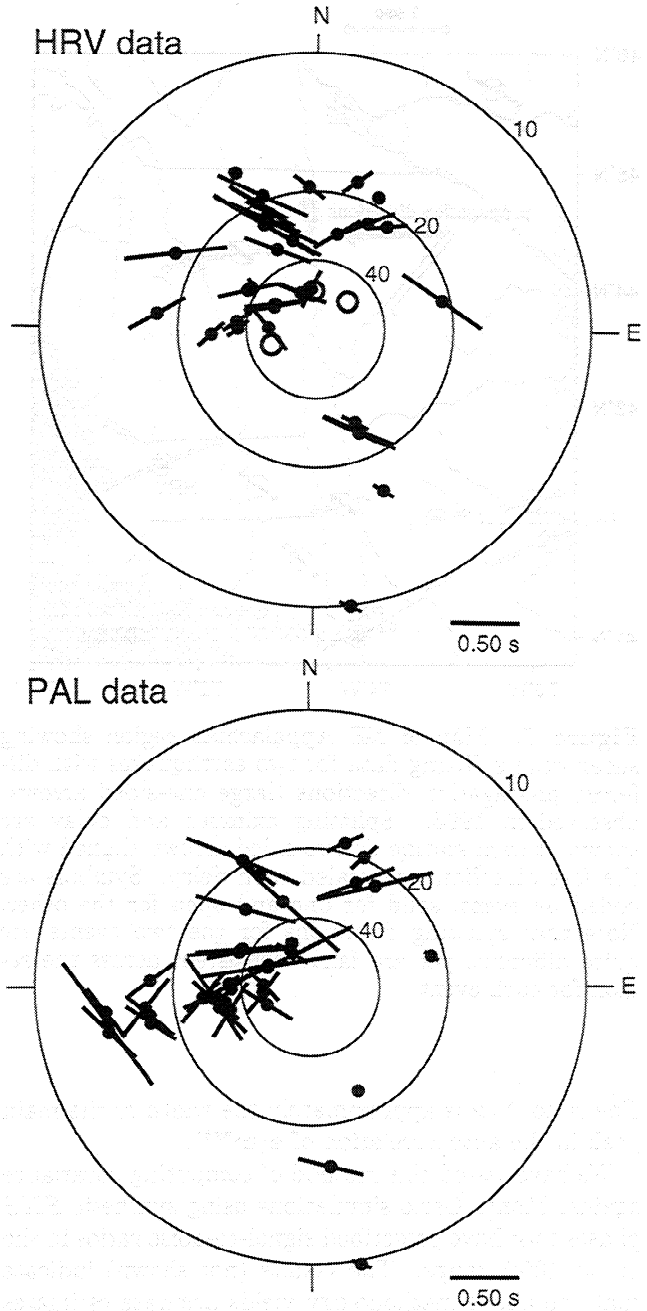

Figure 8. Shear wave splitting data for PAL and HRV. Note that the pattern is similar for the two stations but varies rapidly with back azimuth. Splitting directions for S_{diff} phases (two data points from back azimuth 335° for HRV, three data points from back azimuths 257° – 263° for PAL) closely match those obtained for SKS phases from the same events. Thus contamination of the S_{diff} signal by the D'' anisotropy [*Garnero and Lay*, 1997] does not seem to occur along these particular paths. S phases from South American earthquakes with hypocenters deeper than 500 km are included to provide coverage from the south.

function of back azimuth. Variability is also seen across the region for each event, indicating that some lateral heterogeneity is present. This heterogeneity was characterized by *Levin et al.* [1996] in terms of differences between "Appalachian" and "Grenvillian" provinces.

We compiled SKS splitting data for the two longest running of these stations, HRV (Harvard, Massachusetts) and PAL (Palisades, New York) (Figure 8). We used observations of SKS, $SKKS$ and PKS phases, as well as a few S_{diff} and S phases from deep-focus events. Core phases (SKS and the like) are SV-polarized by the $P - S$ conversion at the core-mantle boundary and are useful for the study of the seismic anisotropy in the upper mantle and lithosphere. In the interest of broadening the azimuthal coverage of our dataset we also used S and S_{diff} phases from medium-sized events with hypocenters deeper than 500 km. We assume that these phases encounter anisotropy only in the "receiver-side" upper mantle and the lithosphere. We also note that splitting parameters obtained for S_{diff} phases (two observations for HRV, three observations for PAL) closely match splitting parameters obtained for SKS phases from same events. Thus potential contamination of the S_{diff} signal by the D'' anisotropy [*Garnero and Lay*, 1997] does not seem strong along these particular paths.

The data for these two stations are quite similar (Figure 9). Fast direction azimuths tend to fall into the northeasterly and easterly populations discussed above, resulting in a bimodal distribution of the azimuthal angle between pairs of measurements (Figure 10). The assumption of two populations (with mean azimuths of N60°E ±4° and N119°E ±2°) is statistically superior to the assumption of only one population (with mean azimuth of N95°E ±5°) at the 99.9% significance level (computed via the F test). The means of these two populations are also different at the 99.9% significance level (computed via the t test). We have examined the SKS

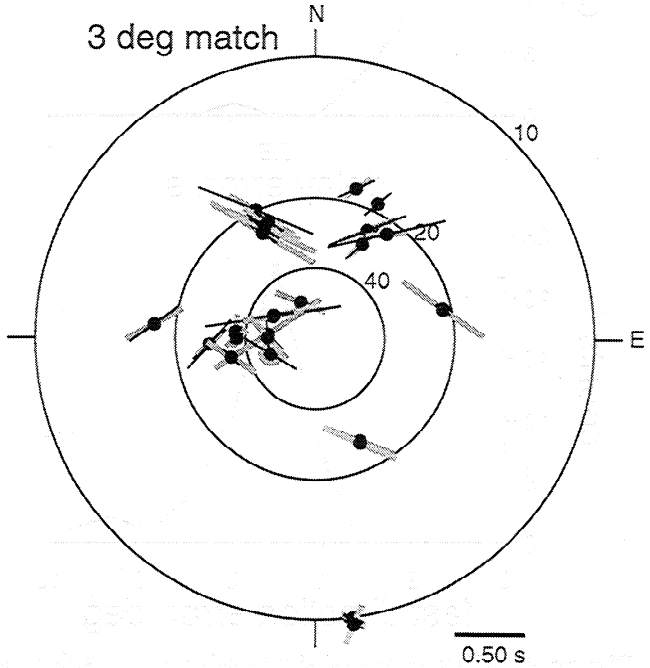

Figure 9. Shear wave splitting data for the subset of PAL and HRV data that fall within 3° of each other, superimposed on one another (solid, HRV; shaded, PAL). Note overall similarity of pattern.

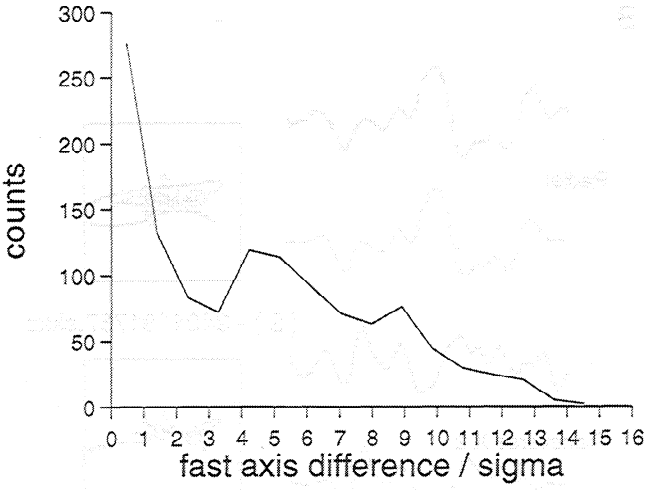

Figure 10. Histogram of the angle between pairs of fast azimuth measurements for the station HRV. The distribution is bimodal, suggesting that two distinct fast azimuths are present.

seismograms that were used as input to the splitting parameter estimation procedure (Figure 11). No anomalies that might cause spurious parameter estimates are apparent, giving us confidence that observed variation of splitting parameters is real.

Barruol et al. [1997] measured shear wave splitting at HRV using several of the earthquakes in our data set. They report ϕ = N86°E (or N89°E), τ = 0.99 s (or 0.65 s) (values given for two different processing techniques). This result is quite similar to our "single population" mean of N95°E. It is interesting to note that the plot of all HRV data of *Barruol et al.* [1997, Figure 5] and their table listing individual values (electronic supplement Table 2) contain members of both populations of fast directions. Another analysis of HRV data was done by *Fouch and Fischer* [1995] to compare with data from the MOMA (Missoury-Masachusetts) portable array, but they included only those events that occurred while the array was active (1995 through early 1996). They reported an average ϕ = N 118°E, τ = 1.13 s, similar to our mean over easterly back-azimuths (N119°E). In both cases the measured average value is biased by the event distribution, which is dominated by northwesterly events from NW Pacific earthquakes. The discrepancy in reported sets of splitting parameters most likely reflects differences in the distribution of data with back azimuth. Although of dubious value given the systematic fluctuations of the data, the mean value of the splitting direction (calculated as a model result, and discussed below) is N89°E, which matches the ϕ value reported by *Barruol et al.* [1997].

We modeled the seismic data using shear wave splitting parameters derived from synthetic seismograms of *SKS* phases. We compared two different algorithms for computing synthetic seismograms in vertically stratified, anisotropic media: a propagator matrix method [*Levin and Park*, 1997b] and a ray method. Both give near-identical results. We use a grid search over anisotropic parameters to find a best-fitting Earth model, where the goodness-of-fit criterion minimizes the misfit

$$E = \sum_i \frac{(\tau_i^{ob} - \tau_i^{pr})^2}{\sigma^2{}_\tau} + \frac{(\phi_i^{ob} - \phi_i^{pr})^2}{\sigma^2{}_\phi}$$

Here τ_i^{ob} and τ_i^{pr} are observed and predicted delay times, ϕ_i^{ob} and ϕ_i^{pr} are observed and predicted fast directions, and σ_τ and σ_ϕ are the standard deviations of the delay time τ and fast direction ϕ, respectively. We have examined two classes of Earth models: one or two anisotropic mantle layers placed between an isotropic crustal layer and an isotropic mantle half-space. We search only for the thickness of the layers and the orientation of the anisotropic tensors. The anisotropic medium is constrained to consist of 30% orthorhombic olivine and 70% isotropic olivine, a mixture that is about 6% anisotropic for shear waves. The best fitting one-layer model has an anisotropic layer that is 58 km thick, and the two-layer model has top and bottom layers that are 60 and 90 km thick, respectively. Parameters for our preferred hexagonally symmetric model are indicated in Table 1. Tensor orientations for our preferred orthorhombic model are indicated in Table 2 and Figure 12. Both hexagonal and orthorhombic two-layer models correctly capture the variation of splitting parameters with back azimuth, while the one-layer models do not. Figure 13 compares results for the one- and two-layer orthorhombic models. The variance reduction of the two-layer model is roughly 3 times greater than the one-layer model, an amount that is statistically significant to the 99% level (computed via the F test). The two-layer orthorhombic model gives fast-axis azimuths of N53° E and N115°E for the bottom and top layers, respectively, which are close to the means of the two observed azimuthal populations. The fast-axis strikes for hexagonal symmetry are only slightly different, at N50°E and N100°E for the bottom and top layers, respectively. However, the symmetry axes are tilted: only 15° above the horizontal in the top mantle layer but 40° below the horizontal in the lower layer.

To test whether the symmetry axis tilts are significant, we compare the observed back-azimuth pattern of the apparent fast direction with those predicted by our hexagonal and orthorhombic models, and also by the two-layer splitting operator of *Silver and Savage* [1994] (Figure 14). To construct the operators, we computed the delays τ_k a vertically incident shear phase would experience in each layer of the orthorhombic and hexagonal models, and used respective fast directions. Predicted patterns are quite similar although, as one would expect, the approximation and synthetics show greatest difference at discontinuities in the pattern, where waveform complexity is the greatest. Also, patterns from forward modeling are only approximately periodic because of the tilts of the anisotropy axes. These viola-

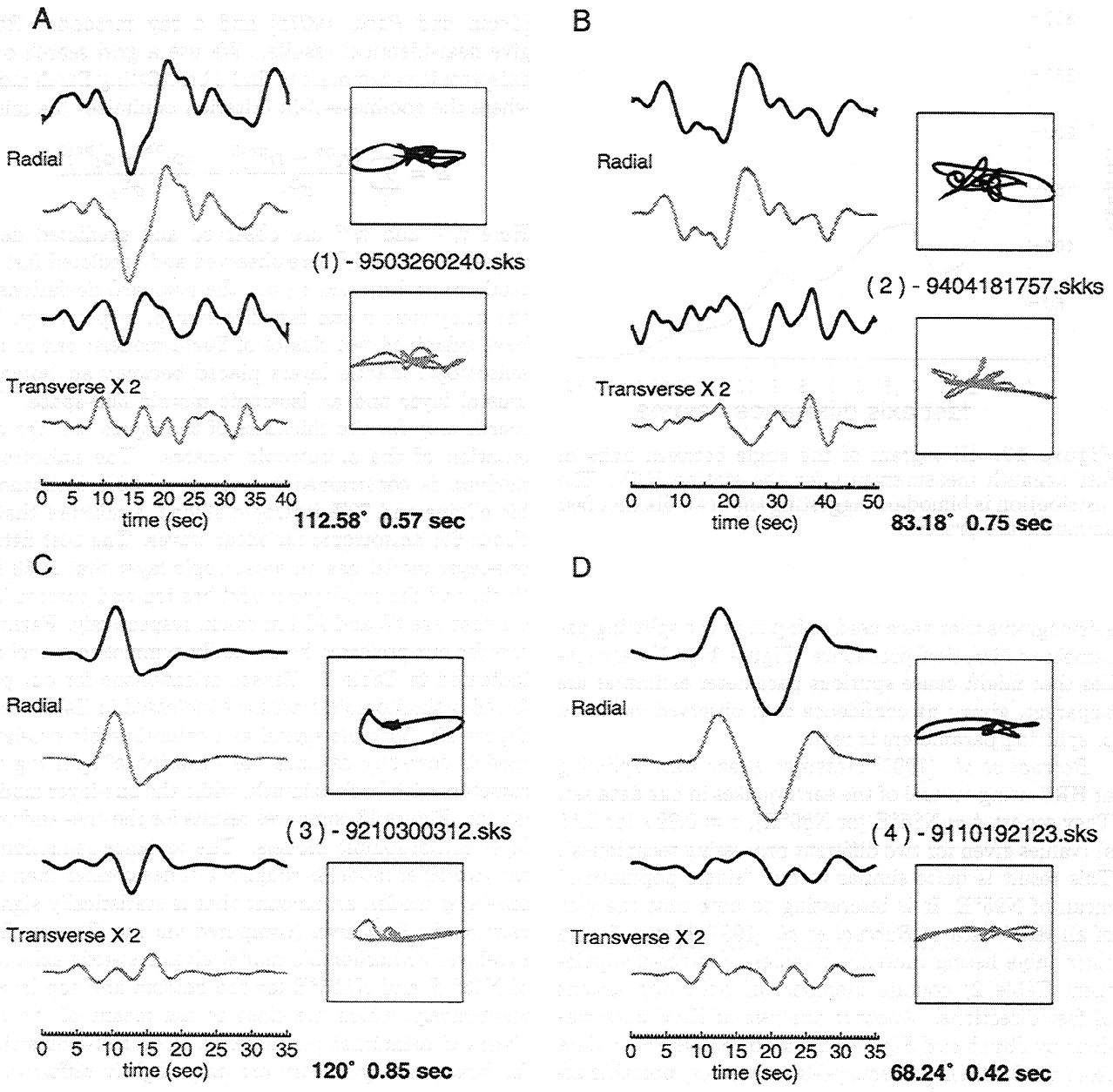

Figure 11. *SKS* waves observed at HRV for four different backaziumths, (a) SSE, (b) WNW, (c) NNW and (d) NNE. (left) Observed radial (top row) and transverse (third row) horizontal component seismograms. The significant energy observed on the transverse component is an effect of the seismic anisotropy. Corrected radial (second row) and transverse (bottom row) component seismograms, where the effect of propagation through the anisotropic medium has been removed. (right) Particle motion diagrams (top) before and (bottom) after correction. Note that the energy on the transverse component has been greatly reduced, and the particle motion made significantly more linear, indicating that the splitting parameters have been correctly calculated.

tions of $\pi/2$ periodicity may possibly serve as diagnostic traits in choosing the preferred model. Our present collection of data is too limited to uniquely resolve the tilt of the symmetry axes, though they seem to prefer some deviation from the horizontal.

The broad spatial coherence of shear wave directions throughout the NE Appalachians (as evidenced in Figure 7) suggest that there is a strong vertical stratification of the anisotropy in the upper mantle beneath that region. Earth models with two anisotropic upper-mantle layers can fit the observed *SKS* splitting data well. More complicated vertically-stratified models cannot be ruled out, but are not required by the data. Some lateral heterogeneity is also present in the splitting data. We note, however, that even large heterogeneity in the splitting data does not necessarily translate into large

Table 1. Anisotropic Structure (Hexagonal Symmetry) Consistent With Shear Wave Splitting Observations at HRV

depth (km)	V_p, km/s	V_s, km/s	ρ, g/cm^3	B,% of V_p	E, % of V_s	θ, deg	ϕ, deg
35	6.00	3.60	2.5	0	0	-	-
135	8.00	4.60	3.1	3	3	75	100
235	8.00	4.60	3.1	4	4	130	50
∞	8.20	4.7	3.3	0	0	-	-

Depth indicates the bottom of each layer. The parameters B and E scale peak-to-peak variations of compressional and shear velocity, respectively, each with $\cos 2\eta$ azimuthal dependence [*Park*, 1996]. The angles θ and ϕ define the tilt (from vertical) and strike (CW from north) of the axis of symmetry within each anisotropic layer.

heterogeneity in structure. Given the quick variation of the parameters with back azimuth, just a few degrees rotation of either the earth model or the incoming shear wave can lead to widely different values of the splitting parameters. A complete characterization of any 3-D "anisotropic domains" responsible for the observed lateral heterogeneity will require extensive back-azimuth coverage at many stations.

We interpret the top anisotropic layer to represent the continental lithosphere associated with the Appalachian orogen, and the bottom layer to represent the asthenosphere. A conceptual model of layered anisotropy under HRV is presented on Figure 15. Alignment of the fast axes of olivine in the upper layer is near-normal to the strike of geomorphological features in New England, where the trend of the Appalachians rotates from northeast to north. The alignment in the lower layer of the model is more in line with the overall strike of the Appalachian Orogen, as well as the hypothetical "edge" of the North American cratonic keel.

5. Shear Wave Splitting at Station ARU in the Foredeep of Urals

The Global Seismic Network station ARU (Arti, Russia) is located on the easternmost edge of the East European platform (Figure 16), in the Uralian foredeep [*Ivanov et al.* 1975; *Zonenshain et al.* 1984] that accumulated sediments in a passive continental margin setting through most of the Paleozoic. The continental collision at the final stage of Uralian orogeny formed an extensive thrust sheet complex to the east of ARU and may also have deformed the sediments underlying ARU. *Levin and Park* [1997a] studied crustal anisotropy beneath ARU using the anisotropic receiver function method. This method, which utilizes $P-S$ conversions in layered media, is sensitive to anisotropy adjacent to interfaces where the conversions occur. *Levin and Park* [1997a] show that receiver function data are consistent with a vertically stratified Earth structure in which both the uppermost and the lower crust are anisotropic, with hexagonal symmetry and strong tilt in the symmetry axes. Unlike typical models of seismic anisotropy in the mantle, the crustal model for ARU contains a layer of anisotropy with a slow symmetry axis. A conceptual model that would exhibit this type of anisotropy is a layer of imbricated peridotite and metapelite lenses in the region of the crust-mantle transition, as described by *Quick et al.* [1995] in the Ivrea deep crustal exposure in the Alps. Upper mantle anisotropy under ARU has previously been studied by *Helffrich et al.*, [1994], who report a mean fast axis strike of N68°E and a splitting time $\tau \sim 1$ s.

We have compiled splitting data from SKS and other core-refracted phases for this station (Figure 17). Several populations of fast-axis strikes are evident. For example, events from the northwest have westerly strike, while those from the east have more northwesterly strike. The best fitting one-layer anisotropic Earth model (Figure 18, top), with fast axis at N73°E azimuth, does not reproduce this pattern well. A combination of the *Levin and Park* [1997a] crustal model with the mantle model of *Helffrich et al.* [1994] does better (not shown), but does poorly at the ENE back azimuths. A model with a second mantle layer improves the fit significantly (Figure 18, bottom). This best fitting model (Table 3) has

Table 2. Anisotropic Structure (Orthorhombic Symmetry) Consistent With Shear Wave Splitting Observations at HRV

Depth, km	V_p, km/s	V_s, km/s	ρ, g/cm^3	θ_f, deg	ϕ_f, deg	θ_i, deg	ϕ_i, deg	θ_s, deg	ϕ_s, deg
40	6.8	3.9	2.85	-	-	-	-	-	
100	8.3	4.8	3.3	89	115	80	25	10	210
190	8.3	4.8	3.3	90	53	67	323	23	143
∞	8.3	4.8	3.3	-	-	-	-	-	

Velocity values in anisotropic layers are the isotropic averages of respective elastic tensors. The anisotropic medium is modeled as 30% orthorhombic olivine and 70% isotropic olivine, a mixture that is ~6% anisotropic. The angles θ and ϕ define the tilt (from vertical) and azimuth (CW from north) of the symmetry axes (fast, intermediate, slow) within each anisotropic layer.

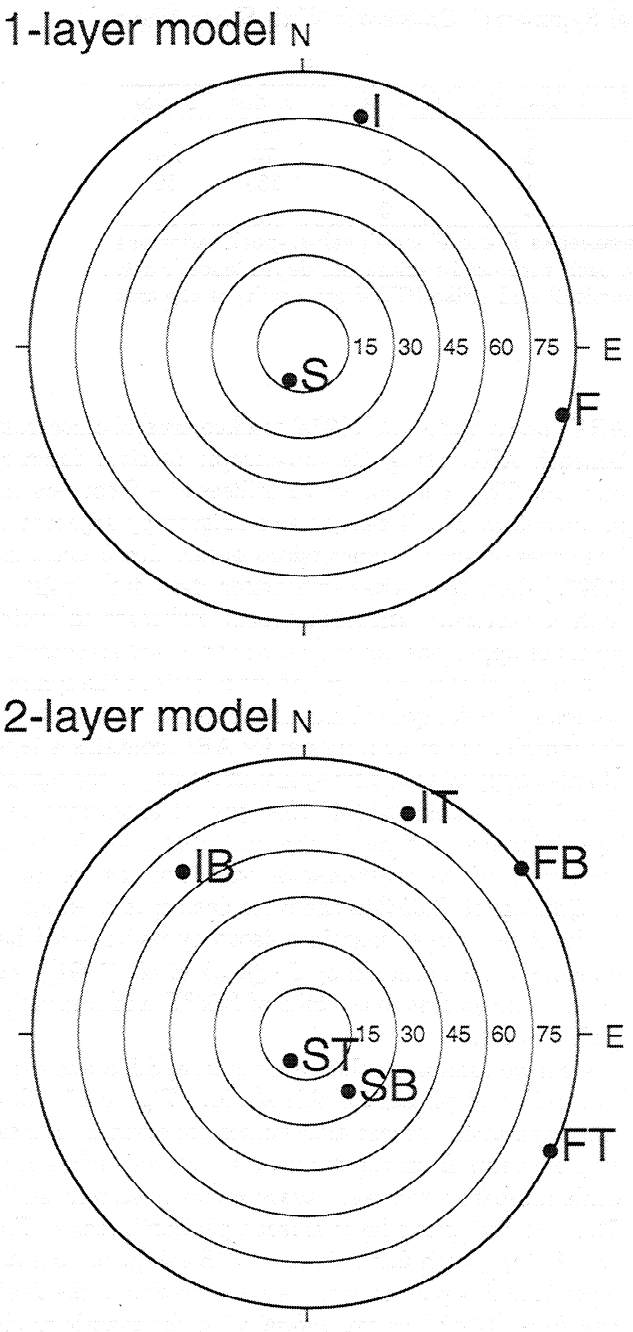

Figure 12. Anisotropic tensor orientations for (top) one-layer and (bottom) two-layer models for HRV. The fast, intermediate, and slow axes are denoted F, I, and S, respectively. Top and bottom layers are denoted T and B, respectively.

a 58 km upper mantle layer with a fast axis striking N50°E atop a 140 km layer with a fast axis plunging 40° to the east (Figure 19).

Figure 20 illustrates a conceptual model of anisotropic layering under ARU. Lower crust and uppermost mantle under the Uralian foredeep are characterized by the common direction of anisotropy $\sim$ 50°, which is significantly oblique to the trend of Urals. It may be related to the deformation within the East European platform that predates the formation of the orogen. The anisotropy-inducing fabric in the lower part of the lithosphere is aligned nearly normal to the strike of the Ural Orogen.

6. Discussion of Geodynamic Implications

In both the Appalachians and the Uralides we find evidence for at least two distinct layers of seismic anisotropy in the mantle. The exact depth and thickness of layers are subject to assumptions about the percent of aligned minerals within the volume. Anisotropic intensities in our models follow measurements done on hand samples of peridotite from ophiolites [*Christensen*, 1984] and are likely to represent the upper bound in percent of alignment. If the alignment of minerals is weaker, the required thicknesses of the anisotropic layers will increase. The tilt of inferred anisotropy-inducing fabric with respect to the horizontal is a function of the symmetry system chosen for the anisotropy. For the Appalachian stations, both orthorhombic anisotropy, with nearly horizontal fast axes, and hexagonal anisotropy, with tilted fast symmetry axes, satisfy the data. We suspect that this trade-off will be common in studies of this type and will be difficult to resolve without a clear indication of the best symmetry choice from mineral texture studies. Significantly, in both modeling exercises the horizontal azimuth of the fast axis does not depend on the symmetry system and the method of computing synthetic seismograms. We thus believe that robust elements of our models are the minimum number of anisotropic layers, their vertical sequence, the orientation of fast direction and the cumulative anisotropy within each of them.

The overall regional consistency of observations in the northeastern Appalachian region (Figure 7) argues against a "local" character for shallow mantle structures revealed by shear wave splitting. Rather, the structure modeled using the HRV data set appears to be common to the area of Appalachian terranes. On the other hand, some regional variation is present [e.g., *Levin et al.*, 1996]. Whether it is caused by the "true" lateral variation in anisotropic features of the subsurface, or simply reflects changes in geometry of observation, is an open question.

In case of the Uralian foredeep we have a "spot" measurement, and arguing for its regional extent is harder. Major geologic structures of the Ural Orogen are very consistent along strike, making it almost two-dimensional. An average splitting direction of 0° (subparallel to the strike of the Urals) reported by *Vinnik et al.*, [1992] at the station SVE near Yekaterinburg (Figure 16) falls on the opposite side of the main Uralian fault zone. This major suture divides accreted terranes from the East European platform [*Zonenshain et al.*, 1984]. The splitting at SVE most likely reflects a different structure in the crust and the uppermost mantle.

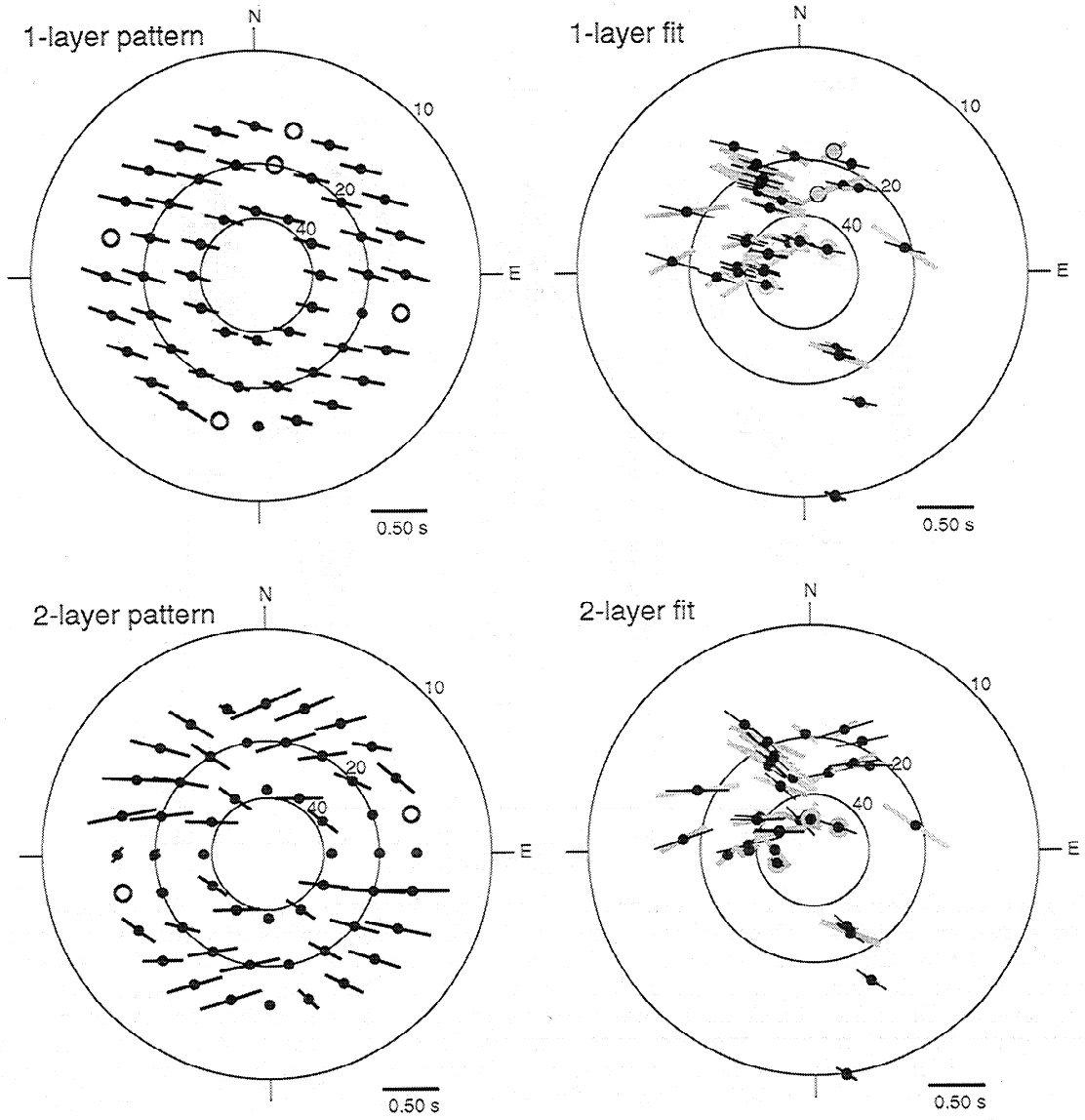

Figure 13. (left) Shear wave splitting patterns for best fitting (top) one-layer and (bottom) two-layer HRV models. (right) Observed (shaded) and predicted (solid) shear wave splitting parameters.

Given the uncertainties discussed above, the interpretation is necessarily tentative. If we consider the anisotropy to be "frozen in" or "fossil", confined within the continental keel, in both Appalachian and Urals we may infer at least two distinct past tectonic episodes. *Abbott* [1991] describes a conceptual model for accumulating material with different deformation fabrics within the body of a continent, via underplating the continent with oceanic plate material during successive episodes of subduction. A similar model, only with oceanic "slabs" stacked in the lateral direction, has been advocated for Western Europe [e.g. *Babuška et al.*, 1993, *Plomerova et al.*, 1996]. The "frozen fabric" explanation appears plausible for the upper layers in both modeled regions. In the Urals the lowermost crust has the same orientation (N50°E, [from *Levin and Park*, 1997a]) as the upper layer of our mantle model. Interestingly, the sense of anisotropy reverses from the crust (slow axis) to the mantle (fast axis). We believe that crustal anisotropy in the crust is imposed by fine layering of materials with contrasting properties, while in the mantle it is imposed by preferred alignment of peridotite minerals. The strike of fabric in lower crust and uppermost mantle under ARU is oblique to the strike of the orogen and may reflect a tectonic episode predating its formation. Analysis of crustal $P-SH$ conversions [*Levin and Park*, 1997b] under HRV did not reveal strong crustal anisotropy of the kind seen under ARU. The upper layer of the mantle anisotropy has fabric orientation that is roughly normal to the geomorphological features and main tectonic boundaries in the region. Numerous subduction episodes, both east verging and west verging,

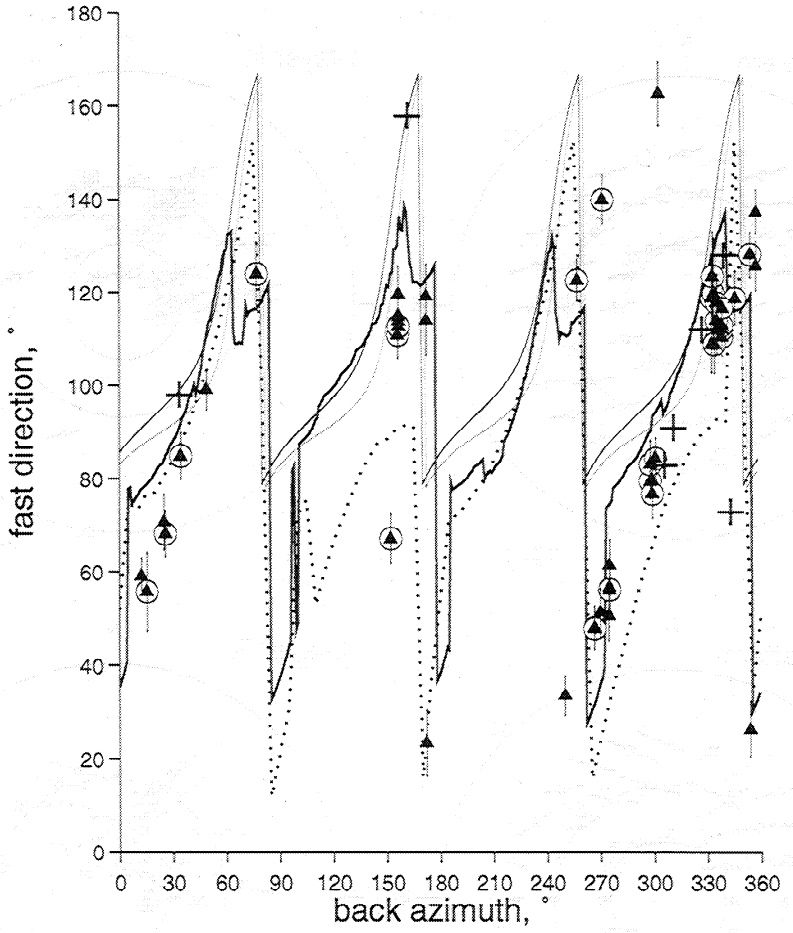

Figure 14. Observed and predicted variation of the apparent fast direction at HRV. Observations are shown by triangles with error bars. A subset of "robust" data points (circled) was chosen so that $\sigma_\tau < \tau/3$. Clearly, robust and "poor" data points follow the same pattern. Crosses show values of fast direction reported for HRV by *Barruol et al.* [1997] (as given in their electronic supplement Table 2). Thick lines show patterns predicted by our orthorhombic (solid) and hexagonal (dotted) models, and thin lines show predictions for equivalent two-layer splitting operators [*Silver and Savage*, 1994]. While all models capture the periodicity of the pattern, the spread of values and the deviations from the 2π pattern are not matched by the splitting operator predictions.

took place during the formation of the Appalachians, and the fabric we reconstruct is likely to be a remnant of one of them.

An alternative mechanism for anisotropy in the mantle, active flow in the asthenosphere [e.g., *Vinnik et al.*, 1992], appears more suitable for the lower layers in our models. For the Appalachians the strike of fabric in the lower layer of our model aligns closely with the absolute plate motion vector of ~N65°E [*Gripp and Gordon*, 1990]. It also aligns with the hypothetical edge of the North American continental keel. The keel edge would direct the orientation of asthenospheric flow if one assumes that mantle moves "west" relative to the North American craton, and around its keel (Fouch et al., submitted manuscript, 1999). The Urals are located in the middle of the Eurasian continent, which is near-stationary with respect to the hot spot reference frame. The direction of possible motion for Eurasia is approximately east-west, if one ignores the error bars on the rate of motion of *Gripp and Gordon*, [1990]. This direction, though poorly constrained, aligns with the fast axis of the lower layer in the anisotropic structure we infer under ARU.

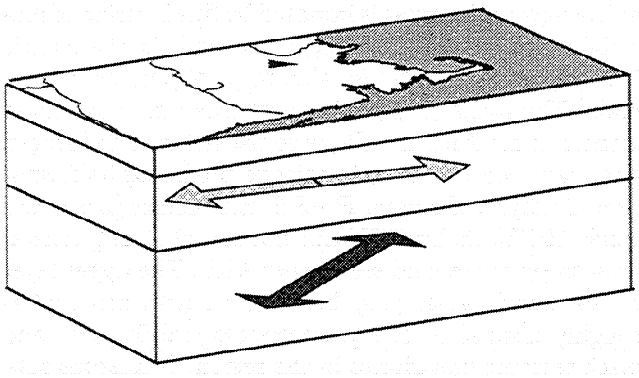

Figure 15. A schematic representation of the model for seismic anisotropy distribution under HRV.

Our results clearly contradict the notion that fast-axis strike for shear wave splitting in a region of com-

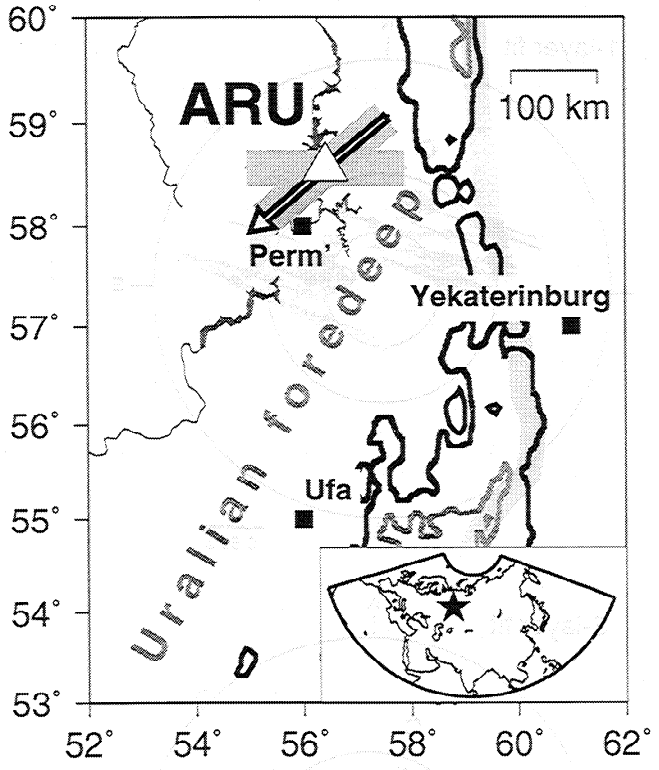

Figure 16. Regional setting of GSN station ARU (open triangle) and the geometry of inferred anisotropy in the lithosphere. Shaded lines, topography contours at 330 and 560 m; wide shaded line, the main Uralian fault zone; open arrow, the symmetry axis of lower-crustal anisotrop; shaded bars, inferred fast axes of anisotropy for the two layers in the mantle.

pressional deformation should align with the strike of the orogen [*Vauchez and Nicolas*, 1991; *Nicolas*, 1993; *Vauchez and Barruol*, 1996]. In two regions of Paleozoic deformation we find patterns of seismic anisotropy consistent with vertically heterogeneous anisotropic structure. It is possible that in such complex regions a subset of measurements will indeed line up with the strike of an orogen. Our experiments with multilayered anisotropic structures show that direct mapping of splitting parameters (or their averages) onto tectonic features can be misleading.

7. Conclusions

Observations of shear wave splitting in the northeastern U. S. Appalachians and in the foredeep of the Urals vary significantly with the back azimuth and incidence angle of the phase. To analyze these data sets properly, we developed a new technique for estimating uncertainties of splitting parameters. Using this technique, we find that typical errors of the shear wave splitting parameters determined from low-passed broadband data from GSN station HRV are 3°-7° for the fast direction and 0.1-0.2 s for the delay.

Experiments with synthetic seismograms generated in simple multilayered anisotropic structures show that splitting parameters tend to vary significantly with the back azimuth of the analyzed shear wave. A restricted subset of back azimuths may strongly bias any model derived from observations, especially if the observations are averaged. On the other hand, the azimuthal variation pattern provides important constraints on vertical or lateral variation of anisotropic properties in the Earth.

On the basis of data from well-recorded events with different back azimuths, splitting parameters appear to be broadly consistent throughout the Appalachian terranes in the northeastern United States. (This consistency weakens for stations west of the Appalachians.) A close similarity in back azimuth dependence of splitting parameters is found in data from two long-running stations in the northeastern United States: HRV and PAL. Good back azimuth coverage at these two stations allows us to separate observations into two statistically significant populations. Within these populations, mean azimuths are N60°E ±4° and N119°E ±2°, and delay values vary within each population from near zero to ~1 s. The exact values of delays, as well as individual estimates of fast direction, are affected by the filter parameters chosen when low passing. The back azimuth dependence of splitting parameters for the station ARU near the Urals is characterized by sharp transitions between different groups of observations.

Using synthetic seismograms computed in flat-layered media we developed one-dimensional models of seismic anisotropy distribution under stations HRV and ARU.

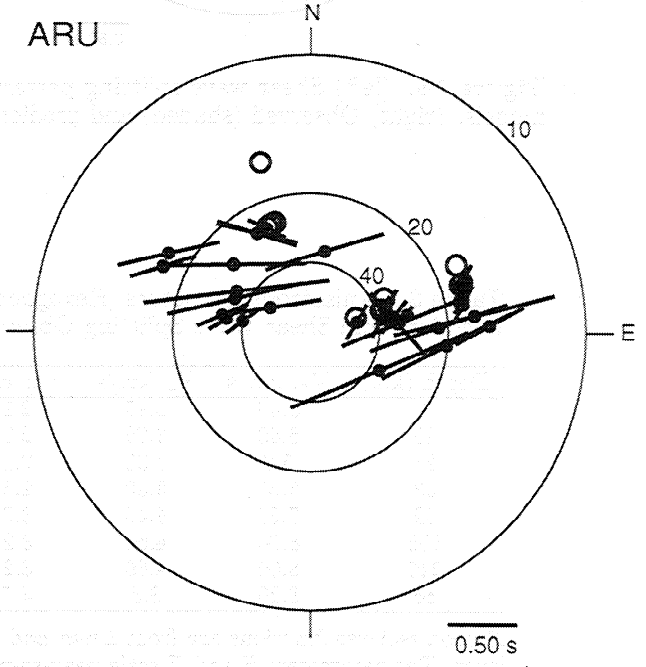

Figure 17. Shear wave splitting data for ARU (Arti, Russia). See Figure 1 for plotting conventions.

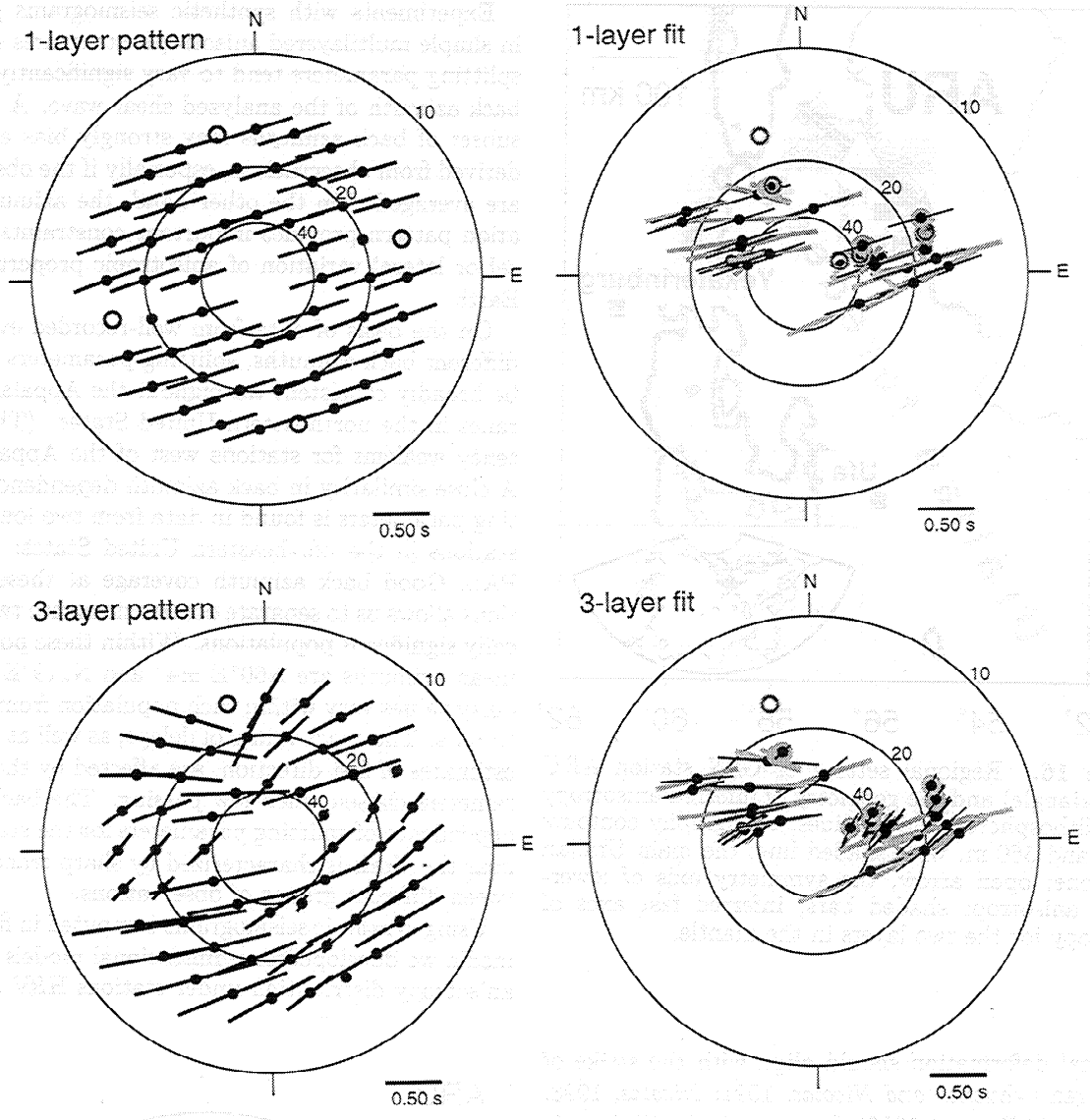

Figure 18. (left) Shear wave splitting patterns for best fitting one-layer and three-layer ARU models. (right) Observed (shaded) and predicted (solid) shear wave splitting parameters.

Table 3. Anisotropic Structure (Hexagonal Symmetry) Consistent With P coda Receiver Functions and Shear Wave Splitting Observations at ARU

Depth (km)	V_p, km/s	V_s, km/s	ρ, g/cm^3	B, % of V_p	E, % of V_s	θ, deg	ϕ, deg
1	5.00	2.95	2.1	-15	0	45	345
20	6.40	3.70	2.3	0	0	-	-
23	5.8	3.30	2.3	0	0	-	-
33	6.60	3.80	2.6	0	0	-	-
42	7.60	4.40	3.0	-15	-15	65	230
100	8.00	4.60	3.2	6	6	80	50
240	8.00	4.60	3.2	4	4	130	90
∞	8.20	3.3	4.7	0	0	-	-

P coda reciever functions are from *Levin and Park* [1997a]. Depth indicates the bottom of each layer. The parameters B and E scale peak-to-peak variations of compressional and shear velocity, respectively, each with $\cos 2\eta$ azimuthal dependence [*Park*, 1996]. The angles θ and ϕ define the tilt (from vertical) and strike (CW from north) of the axis of symmetry within each anisotropic layer.

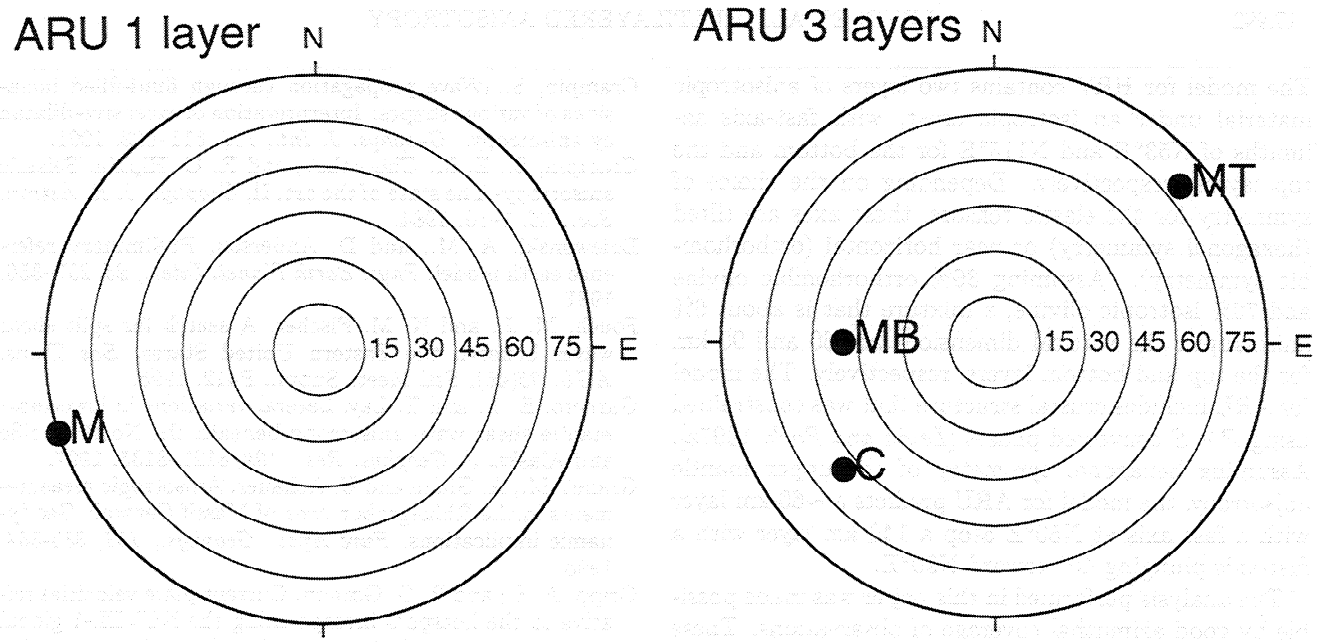

Figure 19. Symmetry axes of best fitting hexagonal tensors for ARU. Crust and mantle are labeled C and M, respectively. Top layer and bottom layers in the mantle are labeled T and B, respectively. In the bottom layer of anisotropy the symmetry axis plunges 40° to the east, which is equivalent to an upward tilt of 40° to the west.

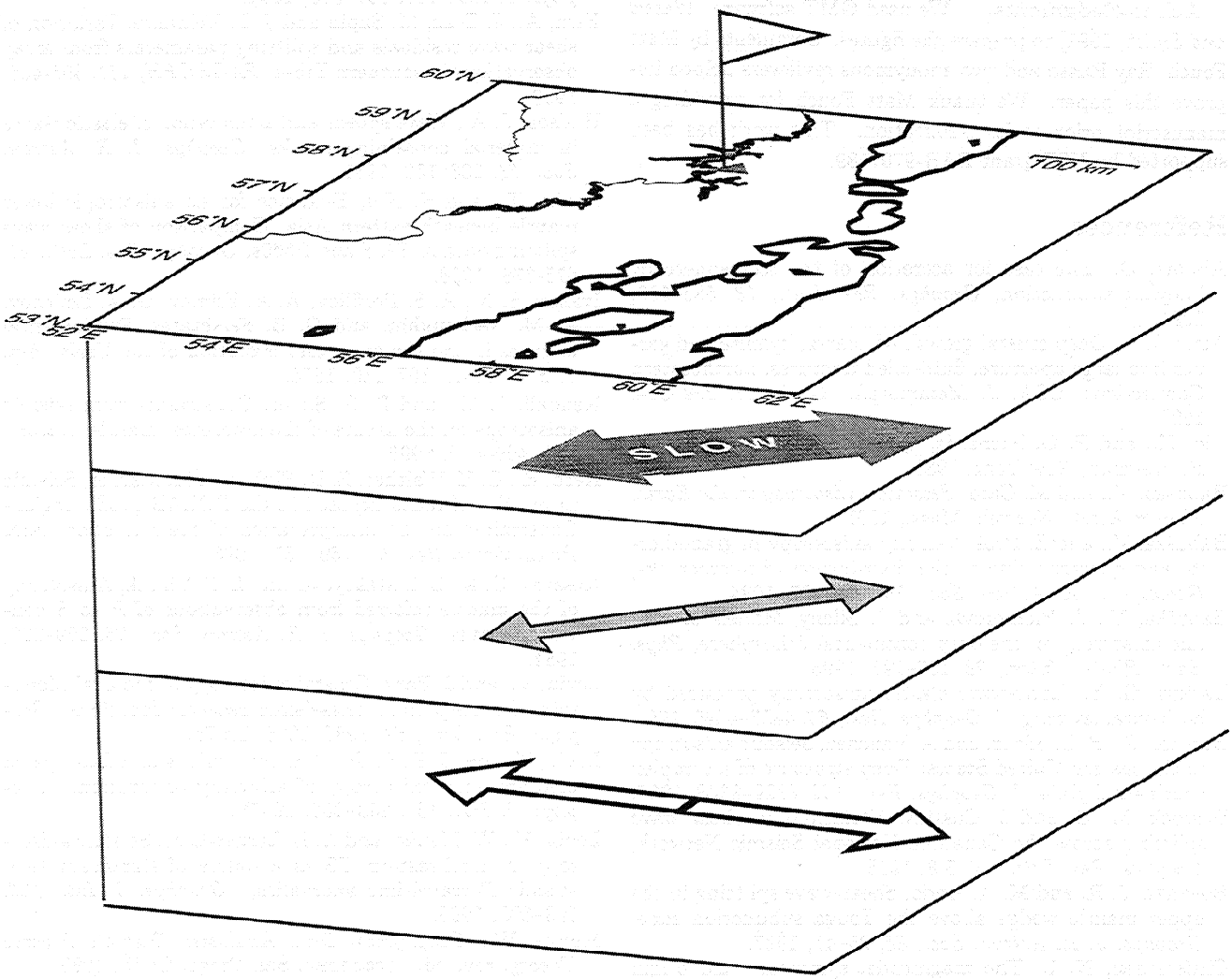

Figure 20. A schematic representation of the model for seismic anisotropy distribution under ARU (marked by flag), with the lowermost crust anisotropy (dark arrow marked slow) from the model of *Levin and Park* [1997a].

The model for HRV contains two layers of anisotropic material under an isotropic crust, with fast-axis azimuths of N53°E and N115°E for the bottom and the top layers, respectively. Depending on the choice of symmetry for the elastic tensors, these axes are tilted (hexagonal symmetry) or near horizontal (orthorhombic symmetry). Assuming 30% orthorhombic olivine and 70% isotropic olivine, a mixture that is about 6% anisotropic, the vertical dimensions are 60 and 90 km for the top and bottom layers, respectively. The model for ARU includes crustal structure that was constrained using $P-S$ converted phases [*Levin and Park*, 1997a]. Assuming hexagonal symmetry of the upper mantle anisotropy, the model for ARU predicts a ~60 km layer with a fast axis at N50°E atop a 140 km layer with a fast-axis plunging 40° toward N90°E.

The analysis performed in this paper was made possible by good azimuthal coverage of observations. These are generally obtainable through prolonged observation. Data from short deployments, even in stable continental regions, apparently run the risk of bias from an uneven distribution of seismicity.

Acknowledgments. We used GMT software [*Wessel and Smith*, 1991] to prepare the figures. Comments by Matt Fouch, Ray Russo and two anonymous reviewers helped improve this paper. We thank Matt Fouch for providing a manuscript prior to its publication. This work has been supported by NSF grant EAR-9707189.

References

Abbott, D., The case for accretion of the tectosphere by buoyant subduction, *Geophys. Res. Lett., 18*, 585–588, 1991.

Ague, J. J., Deep crustal growth of quartz, kyanite and garnet into large aperture, fluid-filled fractures, northeastern Connecticut, USA, *J. Metamorph. Geol., 13*, 299–314, 1995.

Aki, K., and P. G. Richards, *Quantitative Seismology*, W. H. Freeman, New York, 1981.

Babuška, V., and M. Cara, *Seismic Anisotropy in the Earth*, Kluwer Acad., Norwell, Mass., 1991.

Babuška, V., and Z. Proš, Velocity anisotropy in granodiorite and quartzite due to the distribution of microcracks, *Geophys. J. R. Astron. Soc., 76*, 121–127, 1984.

Babuška, V., J. Plomerova, and J. Sileny, Models of seismic anisotropy in the deep continental lithosphere, *Phys. Earth Planet. Inter., 78*, 167–191, 1993.

Backus, G. E., Long-wave elastic anisotropy produced by horizontal layering, *J. Geophys. Res., 67*, 4427–4440, 1962.

Barruol, G., P. G. Silver, and A. Vauchez, Seismic anisotropy in the eastern United States: Deep structure of a complex continental plate, *J. Geophys. Res., 102*, 8329–8348, 1997.

Bostock, M. G. and J. Cassidy, Variations in shear wave splitting across the Canadian National Seismic Network, *Geophys. Res. Lett., 22*, 5-8, 1995.

Bowman, J. R. and M. A. Ando, Shear-wave splitting in the upper mantle wedge above the Tonga subduction zone, *Geophys. J. R. Astron. Soc., 88*, 25–41, 1987.

Christensen, N. I., The magnitude, symmetry and origin of upper mantle anisotropy based on fabric analyses of ultramafic tectonites, *Geophys. J. R. Astron. Soc., 76*, 89–111, 1984.

Crampin, S., Wave propagation through fluid-filled inclusions of various shapes: Interpretation of extensive-dilatancy anisotropy, *Geophys. J. Int., 104*, 611–623, 1991.

Crampin, S., E. M. Chesnokov, and R. G. Hipkin, Seismic anisotropy- The state of the art, II, *Geophys. J. R. Astron. Soc., 76*, 1–16, 1984.

Dziewonski, A. M., and D. Anderson, Preliminary reference earth model, *Phys. Earth Planet. Inter., 25*, 297–356, 1981.

Fouch, M. J., and K. M. Fischer, A search for split shear waves beneath the Eastern United States, *Eos Trans. AGU, 76*(46), Fall Meet. Suppl., F412, 1995.

Garnero, E. J., and T. Lay, Lateral variations in lowermost mantle shear wave anisotropy beneath the North Pacific and Alaska, *J. Geophys. Res., 102*, 8121–8135, 1997.

Granet, M., A. Glahn and U. Achauer, Anisotropic measurements in the Rhinegraben area of Massif Central: Geodynamic implications, *Pure Appl. Geophys., 151*, 333-364, 1998.

Gripp, A. E., and R. G. Gordon, Current plate velocities relative to the hotspots incorporating the NUVEL-1 global plate motion model, *Geophys. Res. Lett., 17*, 1109–1112, 1990.

Helbig, K., *Foundations of Anisotropy for Exploration Seismics*, Elsevier Sci., New York, 1994.

Helffrich, G., P. G. Silver, and H. Given, Shear-wave splitting variation over short spatial scales on continents, *Geophys. J. Int., 119*, 561–573, 1994.

Hirn, A., J. Diaz, M. Sapin and J.-L. Veinante, Variation of shear wave residuals and splitting parameters from array observations in southern Tibet, *PAGEOPH, 151*, 395-405, 1998.

Hudson, J. A., Wave speeds and attenuation of elastic waves in material containing cracks, *Geophys. J. R. Astron. Soc., 64*, 133–150, 1981.

Iidaka, T., and F. Niu, Evidence for an anisotropic lower mantle beneath eastern Asia; Comparison of shear wave splitting data of *SKS* and P660s, *Geophys. Res. Lett., 25*, 675-678. 1998.

Ivanov, S. N., A. S. Perfiliev, A. A. Efimov, G. A. Smirnov, V. M. Necheukhin, and G. B. Fershtater, Fundamental features in the structure and evolution of the Urals, *Am. J. Sci., 275A*, 107–130, 1975.

Kendall, J. M., and P. G. Silver, Constraints from seismic anisotropy on the nature of the lowermost mantle, *Nature, 381*, 409–412, 1996.

Kern, H., C. H. Walther, E. R. Fluh, and M. Marker, Seismic properties of rocks exposed in the POLAR profile region-Constraints on the interpretation of the refraction data. *Precambrian Res. 64*, 169–187, 1993.

Kosarev, G. L., L. I. Makeyeva, and L. P. Vinnik, Anisotropy of the mantle inferred from observations of P to S converted waves, *Geophys. J. R. Astron. Soc., 76*, 209–220, 1984.

Levin, V., and J. Park, Crustal anisotropy in the Ural Mountains foredeep from teleseismic receiver functions, *Geophys. Res. Lett., 24*, 1283–1286, 1997a.

Levin, V., and J. Park, $P-SH$ conversions in a flat-layered medium with anisotropy of arbitrary orientation, *Geophys. J. Int., 131*, 253–266, 1997b.

Levin, V., W. Menke, and A. L. Lerner-Lam, Seismic anisotropy in northeastern US as a source of significant teleseismic P traveltime anomalies, *Geophys. J. Int., 126*, 593–603, 1996.

Menke, W., *Geophysical Data Analysis: Discrete Inverse Theory*, rev. ed., Academic, San Diego, Calif., 1989.

Nicolas, A., Why fast polarization directions of *SKS* seismic waves are parallel to mountain belts, *Phys. Earth Planet. Inter., 78*, 337–342, 1993.

Nicolas, A., F. Boudier, and A. M. Boulier, Mechanism of flow in naturally and experimentally deformed peridotites, *Am. J. Sci., 10*, 853–876, 1973.

Ozalaybey, S., and M. K. Savage, Double-layer anisotropy resolved from S phases, *Geophys. J. Int., 117*, 653-664, 1994.

Park, J., Surface waves in layered anisotropic structures, *Geophys. J. Int., 126*, 173–183, 1996.

Plomerova, J., J. Sileny and V. Babuška, Joint interpretation of upper-mantle anisotropy based on teleseismic P-travel time delays and inversion of shear wave splitting parameters, *Phys. Earth Planet. Inter., 95*, 293–309, 1996.

Quick, J. E., S. Sinigoi and A. Mayer, Emplacement of mantle peridotite in the lower continental crust, Ivrea-Verbano zone, northwest Italy, *Geology, 23*, 739–742, 1995.

Ribe, N., On the relation between seismic anisotropy and finite strain, *J. Geophys. Res., 97*, 8737–8747, 1992.

Rumpker, G. and P. G. Silver, Apparent shear wave splitting parameters in the presence of vertically varying anisotropy, *Geophys. J. Int.*, 790–800, 1998.

Russo, R., and P. G. Silver, Trench-parallel flow beneath the Nasca Plate from seismic anisotropy, *Science, 263*, 1105–1111, 1994.

Schutt, D., E. D. Humphreys, and K. Dueker, Anisotropy of the Yellowstone Hot Spot wake, eastern Snake River Plain, Idaho, *Pure Appl. Geophys., 151* 443-462, 1998.

Silver, P. G., Seismic anisotropy beneath the continents: Probing the depths of geology, *Annu. Rev. Earth Planet. Sci., 24*, 385–432, 1996.

Silver, P. G., and W. W. Chan, Shear-wave splitting and subcontinental mantle deformation, *J. Geophys. Res., 96*, 16429–16454, 1991.

Silver, P. G., and M. K. Savage, The interpretation of shear wave splitting parameters in the presence of two anisotropic layers, *Geophys. J. Int., 119*, 949–963, 1994.

Vauchez A. and G. Barruol, Shear-wave splitting in the Appalachians and Pyrenees: Importance of the inherited tectonic fabric of the lithosphere, *Phys. Earth Planet. Inter., 95*, 127–138, 1996.

Vauchez, A. and A. Nicolas, Mountain building: Strike-parallel motion and mantle anisotropy, *Tectonophysics, 185*, 183–201, 1991.

Vinnik, L. P. and J.-P. Montagner, Shear-wave splitting in the mantle *Ps* phases, *Geophys. Res. Lett., 23*, 2449–2452, 1996.

Vinnik, L. P., L.I. Makeyeva, A. Milev, and A. Y. Usenko, Global patterns of azimuthal anisotropy and deformations in the continental mantle, *Geophys. J. Int., 111*, 433–447, 1992.

Vinnik L. P., V. G. Krishna, R. Kind, P. Bormann, and K. Stammler, Shear-wave splitting in the records of the German Regional Seismic Network, *Geophys. Res. Lett., 21*, 457-460. 1994.

Vinnik, L. P., R. W. E. Green, and L. O. Nicolaysen, Recent deformations of the deep continental root beneath southern Africa, *Nature, 375*, 50-52, 1995.

Wessel, P., and W. H. F. Smith, Free software helps map and display data, *Eos Trans. AGU, 72*, 441, 445-446, 1991.

Wolfe, C. J., and P. G. Silver, Seismic anisotropy of oceanic upper mantle: Shear wave splitting methodologies and observations, *J. Geophys. Res., 103*, 749-771, 1998.

Wolfe, C. J., and S. C. Solomon, Shear-wave splitting and implications for mantle flow beneath the MELT region of the East Pacific Rise, *Science, 280*, 1230-1232, 1998.

Zhang, S., and S. Karato, Lattice preferred orientation of olivine aggregates deformed in simple shear, *Nature, 375*, 774–777, 1995.

Zonenshain, L. P., V. G. Korinevsky, V. G. Kazmin, D. M. Pechersky, V. V. Khain, and V. V. Matveenkov, Plate tectonic model of the South Urals development, *Tectonophysics, 109*, 95–135, 1984.

V. Levin and J. Park, Department of Geology and Geophysics, Box 208109, Yale University, New Haven, CT 06520. (vadim@hess.geology.yale.edu; park@hess.geology.yale.edu)

W. Menke, Lamont-Doherty Earth Observatory, Palisades, NY, 10964. email: menke@ldeo.columbia.edu

(Received August 3, 1998; revised March 10, 1999; accepted May 3, 1999.)